Contents lists available at ScienceDirect

EBioMedicine

Research paper

Intranasal *Bifidobacterium longum* protects against viral-induced lung inflammation and injury in a murine model of lethal influenza infection

David Groeger[a,b,g,*], Elisa Schiavi[a,c], Ray Grant[a], Magdalena Kurnik-Łucka[d], David Michalovich[e], Rick Williamson[e], Soren Beinke[e], Barry Kiely[b], Cezmi A Akdis[c], Edith M Hessel[e], Fergus Shanahan[f], Liam O' Mahony[f]

[a] *Alimentary Health Pharma Davos, Davos, Switzerland*
[b] *PrecisionBiotics Group Ltd., Cork, Ireland*
[c] *Swiss Institute of Allergy and Asthma Research (SIAF), University of Zurich, Davos, Switzerland*
[d] *Department of Pathophysiology, Jagiellonian University Medical College, Krakow, Poland*
[e] *GSK, Stevenage, United Kingdom*
[f] *Department of Medicine and School of Microbiology, APC Microbiome Ireland, National University of Ireland, Cork, Ireland*
[g] *Lead contact*

ARTICLE INFO

ABSTRACT

Background: Prophylactic strategies are urgently needed for prevention of severe inflammatory responses to respiratory viral infections. Bacterial-host interactions may modify the immune response to viral infections.
Methods: We examined the contribution of Intranasal administration of two different *Bifidobacterium longum* strains or its isolated cell wall in controlling viral induced inflammation using a murine model of influenza infection. We monitored mortality and morbidity over a 10-day period and viral load, differential broncho alveolar lavage (BAL) fluid inflammatory cell counts, Lung tissue histology, BAL and serum cytokines, markers of vascular damage and cell death were quantified.
Findings: Intranasal administration of *Bifidobacterium longum* **35624**® or its isolated cell wall prior to virus inoculation significantly reduced viral load within the lungs and significantly improved survival. Reduced viral load was associated with reduced lung injury as suggested by cell death and vascular leakage markers, a shift from neutrophil to macrophage recruitment, reduced inflammatory cytokine levels (including IL-6), reduced type 1 and 2 interferon levels, but increased levels of interferon-λ and surfactant protein D. These protective effects were maintained when the bifidobacterial cell wall preparation was administered 24 h after viral inoculation. The protective effects were also observed for the *Bifidobacterium longum* **PB-VIR**™ strain.
Interpretation: Exposure to these bifidobacterial strains protect against the inflammatory sequelae and damage associated with uncontrolled viral replication within the lung.
Funding: This work has been funded, in part, by a research grant from GlaxoSmithKline, PrecisionBiotics Group Ltd., Swiss National Science Foundation grants (project numbers CRSII3_154488, 310030_144219, 310030_127356 and 310030_144219) and Christine Kühne – Center for Allergy Research and Education (CK-CARE).

1. Introduction

Respiratory viral infections are common but are usually successfully cleared by an appropriate host immune response. A minority of individuals with pre-existing lung disease, other co-morbidities and the elderly are susceptible to severe disease or secondary infections. An important contributor to mortality in vulnerable individuals is acute respiratory distress syndrome (ARDS) which appears to be due to an exaggerated or dysregulated immune response to a certain viral infections including influenza infection [1]. Unfortunately, a predictive biomarker for those likely to experience mild versus life-threatening disease in response to the same virus is not yet available. In the interim, an alternative or complementary approach may be to mobilise the upper respiratory tract immune system via modifications of the local microbial ecosystem.

Accumulating evidence suggests that indigenous bacteria or their components may have distinct effects on mucosal immunity, varying

* Corresponding author.
  E-mail address: dgroeger@precisionbiotics.com (D. Groeger).

from immunomodulatory or immunostimulatory properties depending on the individual strain and environment [2−4]. The immune response to commensal microbes is not simply a form of host defense but represents an intimate and sophisticated bidirectional communications platform that ensures a stable microenvironment is maintained with important symbiotic physiological effects on the host. An effective immune response is one that effectively reduces the viral load, with limited collateral damage to lung tissue, and without an excessive or aberrant inflammatory reaction. Exposure of respiratory immune cells to specific microbiota-associated regulatory signals may dampen the aberrant inflammatory response and support efficient clearance of the virus [5-8].

One immunoregulatory microbe is the *B. longum* **35624** strain, which has been shown to mitigate pro-inflammatory responses to bacterial infection by induction of tolerogenic immune responses within the gastrointestinal tract in murine and human studies [9-12]. Some, but not all, of these immunoregulatory properties have been attributed to an exopolysaccharide (EPS) which may dampen inflammatory responses in the lung and limit allergen-induced eosinophil infiltration [13-15]. While *bifidobacteria* are usually associated with the gastrointestinal tract, immunomodulatory metabolites or bifidobacterial cell wall components are likely to engage the immune system, regardless of the mucosal site to which they are exposed.

We have assessed the *B. longum* **35624** strain and its isolated cell wall for protective effects *in vivo* in a murine model of lethal influenza infection. The results show that intra-nasal administration reduces viral replication in the lung, protects against lung damage and enhances survival. These effects are associated with an interferon-λ and surfactant protein D response.

2. Materials and methods

2.1. Mice and infection model

Female 7-week-old BALB/c mice (Specified Pathogen Free; SPF) were purchased from Charles River Laboratories (l' Arbresle Cedex, France). All mice were housed in Preclin Biosystems AG (Epalinges, Switzerland). Mice were randomly allocated to 5 animals per cage in individually ventilated cages in a 12/12 h light/dark cycle with food and water available ad libitum and cage enrichment was present. Mice were monitored daily and acclimatized to facility for 7 days prior to initiation of study (Study Day 0). Daily care of the animals was performed. 8-week-old female mice were used for all experiments. Mice from the same litter and co-housed were randomly allocated to different treatment groups prior to start of experiment, to avoid subjective bias of allocating mice into treatment groups after symptom onset. Investigators were blinded to the identity of the treatment groups until data analysis. Influenza virus strain PR8 (A/Puerto Rico8/34, H1N1) was obtained from Virpur (San Diego, CA). The initial PR8 stock concentration was ($1 \times 10e8$ pfu/ml) and it was stored frozen in aliquots. When required these aliquots were thawed and diluted in phosphate-buffered saline (PBS) to 100 PFU/50 μl which was then administered intranasally to the mice for all viral infection experiments. For the viral challenge the mice were anaesthetized by intraperitoneal injection with 9.75 mg Xylasol and 48.75 mg Ketasol per kg body weight and each animal received 50 μl virus solution by intranasal inoculation. All animal experiments were approved by and performed in strict accordance of the Institutional Ethics Committee of Animal Care of Preclin Biosystems AG (Epalinges, Switzerland) and the GSK Policy on the Care, Welfare and Treatment of Animal. These experiments were approved under the local authorization license number VD2830 (issued and approved by: Service de la consommation et des affaires vétérinaires du Canton de Vaud).

2.2. Bacterial cultures

A glycerol stock culture of *B. longum* **35624**® was provided by PrecisionBiotics Limited. It was thawed and inoculated into 10 ml of de Man Rogosa and Sharpe medium (MRS; Oxoid Ltd., Basingstoke, Hampshire, United Kingdom) supplemented with 0.05% cysteine-HCl and incubated for 24 h at 37 °C under anaerobic conditions. This was then inoculated into 50 ml of broth, and after 24 h then inoculated into 250 ml for a further 48 h. Freeze dried *B. longum* **35624**® strain and *B. longum* **PB-VIR**™ strain were supplied by PrecisionBiotics Limited.

2.3. B. longum **35624**® cell wall fraction

The bacterial cell wall (CW) were prepared as described briefly below. The cells (total cell count 1.5 $\times$ 10^{11}) were centrifuged at 14,000 rpm, with the JA-20 rotor (Avanti J-26 x P Beckman Coulter)

for 20 min at 4 °C. The cells were washed three times with sterile phosphate buffered saline (PBS) pH 7.0. The pelleted cells were resuspended in 50 ml of PBS and were incubated with a chelating agent EDTA (final concentration 5 mM) (Fluka) followed by two freeze thaw cycles in liquid nitrogen. The cells were subjected to enzymatic treatment with a glycoside hydrolase lysozyme (Sigma 10 mg/ml) and/ or N acetylmuramidase mutanolysin (Sigma 2.5KU) for 1 hour at 37 °C with occasional agitation by vortexing. Finally, the cells were disrupted using a Sonicator (VibraCell SONICS) with sterile glass beads (90−150 μm particle size (VWR)) for 90 mins. Sonication cycles were stopped when there was disruption to over 95% of the cells as determined by microscopy. The beads were allowed to settle, and after centrifugation at 14,000 rpm for 20 min, the supernatant was removed. The cell wall fraction was removed from the top layer of sediment and was further purified by 4 rounds of resuspension in PBS and centrifugation at 14,000 rpm for 20 min. The final solution was sterilized by filtration using 0.45 μm pore size filters (Millipore Corp., Bedford, Mass.) and further purified by filtration using a 100 kDa MWCO UF device (Millipore Corp). The final dry weight of the cell wall fraction was 30 mg/ml.

2.4. Bacterial treatments in the infection model

Mice were anesthetized using a calibrated vaporizer system (VIP300, Provet, Vet.Med Center, Lyssach, CH) delivering the anesthetic agent, isofluoran (Provet AG,) into a plexiglas chamber containing the mice. Anesthetized animals were administered a total volume of 50 μl of *B. longum* **35624** strain cells (10^9 total) or *B. longum* **35624** strain cell wall fraction (150 mg/ml or 7.5 mg/50 μl) or vehicle (PBS) intranasally, as trickled over both nostrils using a 100 ul Gilson pipette. In the dose response experiment, the *B. longum* **35624** strain cell wall fraction was diluted from the highest dose of 7.5 mg/50 μl, to 0.75 mg/50 μl, 0.25 mg/50 μl, 0.075 mg/50 μl and 0.0075 mg/ 50 μl. This was administered at −2 h, +1 day, +3 days and +5 days post viral inoculation on Day 0. Uninfected vehicle controls were included by administering the vehicle control on day +1 and day +3, but without the PR8 influenza intranasal inoculation. Uninfected and untreated controls were included as the 0 days measurement. Endotoxin levels of the cell wall fraction were 0.6EU/ml (0.03EU per 50 ul) as assessed by the PyroGene Recombinant Factor C Assay (Lonza).

Animals were monitored daily for morbidity (including temperature, and clinical score). Temperatures were recorded rectally utilizing a Microtherma 2 Type "T" Thermometer (TW2−193). While the Clinical Criteria were scored as follow:

1 point for a healthy mouse; 2 points for a mouse showing signs of malaise, including slight piloerection, slightly changed gait and increased ambulation; 3 points for a mouse showing signs of strong piloerection, constricted abdomen, changed gait, periods of inactivity; 4 points for a mouse with enhanced characteristics of the previous group, but showing little activity and becoming moribund; 5 points for a deceased mouse. Mice were euthanized when they reached clinical score greater than 4 or a temperature of less than 33 °C, whichever came first.

On Days 0, 3, 5 and 10 mice underwent bronchoalveolar lavage (BAL) for BAL cytometry and for measurement of cytokines and markers of cell death and vascular leakage. A subset of animals was sacrificed on Days 0, 3, 5 and 10 for phlebotomy, organ removal and analysis. Viral levels in lung tissue (half of all lung lobes) was quantified by quantitative PCR (qPCR). For a subset of animals, the collected lung tissue (half lung lobes) was snap-frozen for histology and stored frozen at −80 °C.

In specific experiments, the therapeutic effects of *B. longum* **35624** cell wall was determined by administration post-infection on day +1 and day +3. Uninfected Vehicle controls were included by administering the vehicle control on day +1 and day +3, but without the PR8 influenza intranasal inoculation. In some experiments, the efficacy of

another *B. longum* strain, *B. longum* **PB-VIR™** (10^9 total) was assessed by administration at −2 h, +1day, +3days.

2.5. Measurement of viral levels in lung tissue

Total RNA was purified from isolated lung lobes using TRI Reagent (Molecular Research centre) and then treated with DNase (Invitrogen) to avoid genomic DNA contamination. RNA was reverse transcribed to cDNA using SuperScript III (Invitrogen). cDNA was quantified by real-time PCR (iCycler; Bio-Rad) using SYBR Green (Stratagene) and samples were normalized to GAPDH expression levels. Primer sequences (forward and reverse, respectively) used were influenza PR8 Matrix protein, 5′-GGACTGCAGCGTAGACGCTT-3′ and 5′CATCCTGTATATGAGGCCCAT-3′.

2.6. Broncho-alveolar lavage (BAL)

Broncho-alveolar lavage (BAL) was performed using 500 ul of PBS supplemented with 0.2% BSA. Total cell numbers in the BAL were determined using a Coulter Counter (IG Instrumenten-Gesellschaft AG, Basel, Switzerland). Differential cell counts were performed on cytospins stained with Diff-Quik solution (Dade Behring, Siemens Healthcare Diagnostics, Deerfield, IL). Percentages of eosinophils, neutrophils, macrophages and lymphocytes were determined by counting 200 cells per sample.

2.7. Histology

Lung tissue was fixed in 10% neutral-buffered formaldehyde and paraffin embedded under standard conditions. Tissue sections (5 μm) were stained with haematoxylin and eosin (H&E) with a standard protocol. Qualitative assessments were performed by a blinded observer. Representative photomicrographs (600x) were taken to illustrate the major distinguishing morphological features among the experimental groups.

2.8. Measurements of cytokines and chemokines

The concentrations of murine IL-1β, IL-2, IL-4, IL-5, IL-6, IL-9, IL-10, IL-12p70, IL-12/IL-23p40, IL-13, IL-15, IL-16, IL-17A, IL-17A/F, IL-17C, IL-17E, IL-17F, IL-21, IL-22, IL-23, IL-30, IL-31, IL-33, IP-10, MIP3α, MIP-2, MIP-1β, MIP-1α, MCP-1, KC/GRO, TNF-α, VEGF, EPO, GM-CSF, IFN-γ in both serum and BAL fluid were measured using a U-PLEX Biomarker Group 1 Mouse 35-Plex kit (MesoScale Discovery) following the manufacturers' instructions. ELISA kits were used to measure levels of murine IL-28 (IFN-λ 2/3), G-CSF, TRAIL and AREG (RayBiotech, Inc,), oncostatin M and surfactant protein D (SP-D) (R&D Systems), IFN-α (ThermoFisher Scientific) and IFN-β (PBL Assay Science).

2.9. Markers of lung injury

Vascular leakage into BAL fluid was assessed using a mouse serum albumin ELISA Quantitation Set (Bethyl Laboratories, Inc., Montgomery, TX). To measure cell death, lactate dehydrogenase (LDH) activity was quantified using an LDH assay (Sigma-Aldrich). This assay was performed in a 96-well plate for 30 min according to the manufacturer's instructions and analyzed using the MicroTek plate reader (Bio-Rad, Hercules, CA).

2.10. Statistical analysis

Graphing and statistical analysis were performed using Prism 8 (GraphPad software, San Diego, CA, USA). Treatment group sample sizes were designed to give statistical power, while minimizing animal use. For *in vivo* experiments, treatment groups of n = 5 were

standard, and results from three experiments were pooled for day 5 viral load measurement, survival analysis, clinical score, and rectal temperature to increase power. All the time course data was expressed as the mean ± SEM or as box-and-whisker plots with the median values and maximum/minimum values for day 5 analysis. Survival differences were assessed by Log-rank (Mantel Cox). The differences between two groups were analysed for significance using the Mann-Whitney test. Intergroup differences were assessed by one-way analysis of variance (ANOVA) followed by post hoc analysis (Dunnett's multiple comparisons test). Time course differences between 2 groups were assessed by two-way ANOVA followed by post hoc analysis (Sidak's multiple comparisons test. For overall daily clinical and rectal temperature curves the p values were calculated using area under the curve analysis with unpaired t-test with Welch's correction.

3. Results

3.1. Intranasal B. longum *35624*® enhances survival in a murine influenza model

The experimental outline is shown in a. Intranasal administration of *B. longum* **35624** intact cells or the strain-derived cell wall fraction prior to and after influenza inoculation reduced viral load in lung tissue compared with controls ($p<0.0001$ n = 15 per group one-way ANOVA) at 5 days post viral inoculation (Fig. 1b). The reduction in viral load was associated with improved survival with 53% of the mice who received the cell wall fraction surviving up to 10 days, compared to 0% survival in control infected mice given vehicle alone (p = 0.0011, n = 15 per group Mantel Cox test) (Fig. 1c). Improved survival of the cell wall fraction-treated versus intact cell-treated animals may be dose related or due to selective purification of protective factors associated with the cell wall. Subsequent experiments focused on animals treated with the cell wall. In agreement with the beneficial effects of the cell wall fraction on survival there was a significant improvement in both clinical score and rectal temperature in later timepoints especially (supplementary Figure. 1a-b). There was a time-dependent increase in viral load in vehicle control infected animals, which was reduced at all time points in the cell wall treated mice. (Fig. 1d). The reduction in viral load by the cell wall fraction was dose-dependent (Fig. 1e).

To exclude the possibility that the survival benefit from intranasal administration of the bifidobacterial strain or cell wall component might be due to non-specific factors such as a change in the pH of the nasal cavity, the cell wall was also administered +1- and +3-days post-inoculation with the virus. The bacterial-derived cell wall treatment administered post-virus inoculation conferred protection and was associated with reduced viral loads at day 5 similar to the levels observed in mice receiving the bifidobacterial cell wall prior to infection (supplementary Figure. 2). At day 9 post inoculation of the virus, 0 of 5 control animals had survived, while 3 of 5 animals in the group administered the cell wall after virus infection had survived.

3.2. B. longum *35624*® cell wall alters the cellular profile of BAL and reduces lung injury

In addition to improved survival and reduced viral load, intranasal administration of *B. longum* **35624** strain-derived cell wall was also associated with a time-dependent alteration in the cellular profile of immune cells within broncho alveolar lavages (BALs). A modest increase in neutrophils was observed in both groups at day 3 post-influenza inoculation, with a further significant increase in neutrophils observed in vehicle-treated animals at day 5, but not in the bacterial-derived cell wall treated mice (Fig. 2a). Macrophages, eosinophils and lymphocytes increased in number at day 5, with macrophages being the numerically dominant population by day 10

in those mice that survived infection (Fig. 2a-d). Supplementary Table 1 illustrates neutrophil and macrophage numbers with 95% CI. In representative lung tissue sections, the perivascular, peribronchial and alveolar immune cell infiltrate was clearly observed in influenza infected animals. An increase in neutrophils (red arrows) was particularly evident in vehicle control-treated animals while macrophages (blue arrows) were present in *B. longum* **35624** cell wall treated animals (Fig. 3a-d). The impact of intra-nasal *B. longum* **35,624** strain-derived cell wall on BAL cell phenotypes was dose-dependent (supplementary Figure 3a-d).

Acute lung injury as shown by cell death and vascular leakage associated with viral replication and inflammatory damage was determined. Both lactate dehydrogenase (LDH) and albumin levels in BAL were significantly increased following 5 days of viral infection but were significantly reduced in the *B. longum* **35624** strain-derived cell wall fraction treated animals (Fig. 4a-b). It is noteworthy that the reduction in these markers was also observed in mice administered the bifidobacterial cell wall preparation 1-day post-inoculation of the virus in addition to those animals that were pre-treated with the cell wall fraction (Fig. 4a-b).

3.3. B. longum *35624*® cell wall exposure modifies cytokine responses in the lung

The dynamic nature of the inflammatory response is reflected in the differences in cytokines, chemokines and surfactant protein D (SP-D) over the course of the infection (Figs. 5 and 6). Altered levels of 42 cytokines and chemokines and SP-D were detected in the BAL samples when measured at day 3 or day 5 virus post-inoculation. These included the interferons (IFN-α, IFN-β, IFN-γ, IFN-λ), chemokines (KC/GRO, MIP3α, MCP-1. MIP-2, IP-10), hematopoietic growth factors (GM-CSF, EPO) and cytokines (IL-4, IL-5, IL-6, IL-10, IL-12, IL-30) (Figs. 5 and 6 (heatmap and representative graphs) and supplementary Figure 3a-h). In particular, intra-nasal administration of the bifidobacterial cell wall preparation was associated with an early protective interferon lambda (IFN-λ) and SP-D response at day 3 post-infection in BALs with a reduction in the interferons (IFN-α, IFN-β, IFN-γ), cytokines and chemokines (IP-10, IL-6 and MCP-1) at day 5 post-infection when compared to the control (vehicle-treated) animals (Fig. 6a-h). A similar reduced level of cytokines and chemokines was observed at day 5 for animals administered the isolated cell wall 1 day following inoculation with influenza virus (supplementary Figure 4a-h).

Concurrent with the changes in BAL, serum levels of IFN-λ and SP-D were increased, while serum IL-6 and IP-10 levels were decreased at day 5 post-infection in mice pre-treated with the cell wall isolated from *B. longum* **35624** in comparison with controls (supplementary Figure 5a-h). The increase in SP-D serum levels was dose-dependent and administration of the cell wall fraction 24 h after influenza inoculation had a similar effect on serum SP-D levels (supplementary Figure 6a-b).

3.4. Bifidobacterial-mediated protection is not restricted to B. longum *35624*®

In order to determine if another *B. longum* strain might also induce similar effects, we administered *B. longum* **PB-VIR**^{TM} strain using the same protocol as described above. This microbe also improved murine survival, with 60% of recipients surviving compared to 0% survival in control infected mice given vehicle alone (Fig. 7a) (p = 0.0203 n = 5 per group Mantel Cox test). Improved survival in the bifidobacterial-treated mice was associated with reduced viral loads ($p>0.001$ n = 5 per group one way ANOVA) (Fig. 7b), an increase in BAL macrophage counts (Fig. 7c), reduced BAL albumin, IFN-α and IFN-β levels (Fig. 7d-f), and an increase in serum SP-D levels (Fig. 7g) compared with the controls at 5 days post influenza inoculation.

a

Experimental design

b

Viral load

c

Survival

d

Time course of infection

e

Dose-dependent response
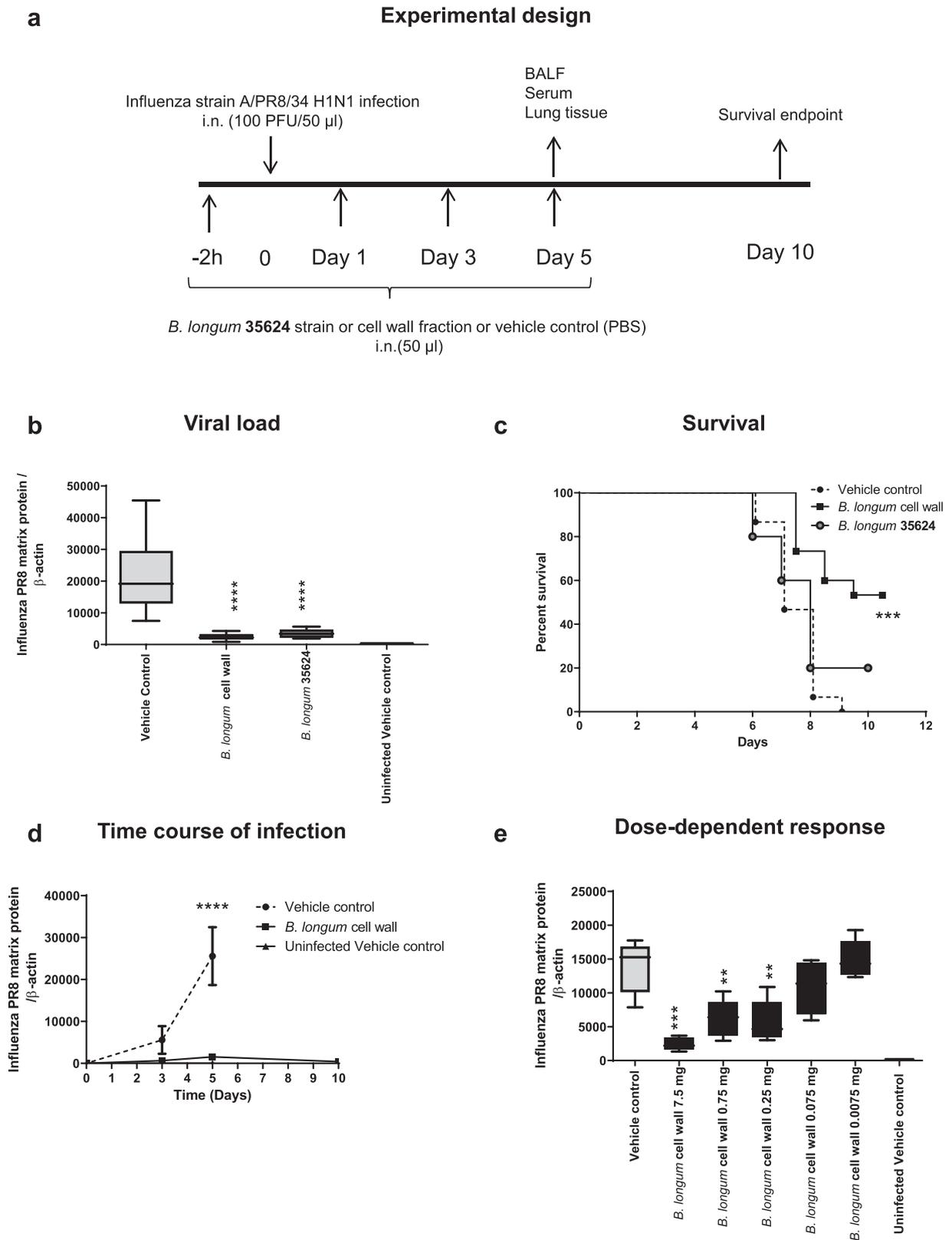
Fig. 1. *Intranasal B. longum* **35624**® *protects against lethal influenza infection.*

(**a**) Experimental model outline for infection with 100 plaque forming units (PFU) of strain A/PR8/34 H1N1 at time 0, following intranasal administration of *B. longum* **35624** bacterial cells, its isolated cell wall, or the vehicle control, at 2 h pre-infection and days 1, 3 and 5 post innoculation. (**b**) Viral load at day 5 post-innoculation in lung tissue as determined by quantitative real-time PCR (viral matrix protein normalized to β-actin expression). Data are presented as box-and-whisker plots with the median values and maximum/minimum values illustrated of 5 animals per group. ****$p < 0.0001$ (1-way ANOVA). (**c**) Survival was monitored up to 10 days post-innoculation ($n = 5-15$ animals per group). ***$p < 0.001$ (log-rank Mantel-Cox test). (**d**) Lung tissue viral load was determined at days 3, 5 and 10 post-innoculation. Data shown are mean ± SEM results of 5 animals per group for each time point. ****$p < 0.0001$ (2-way ANOVA). (**e**) Lung tissue viral load was determined at 5 days post-innoculation in animals administered different doses of isolated cell wall. Data are presented as box-and-whisker plots with the median values and maximum/minimum values illustrated of 5 animals per group. ***$p < 0.001$; **$p < 0.01$ (1-way ANOVA).
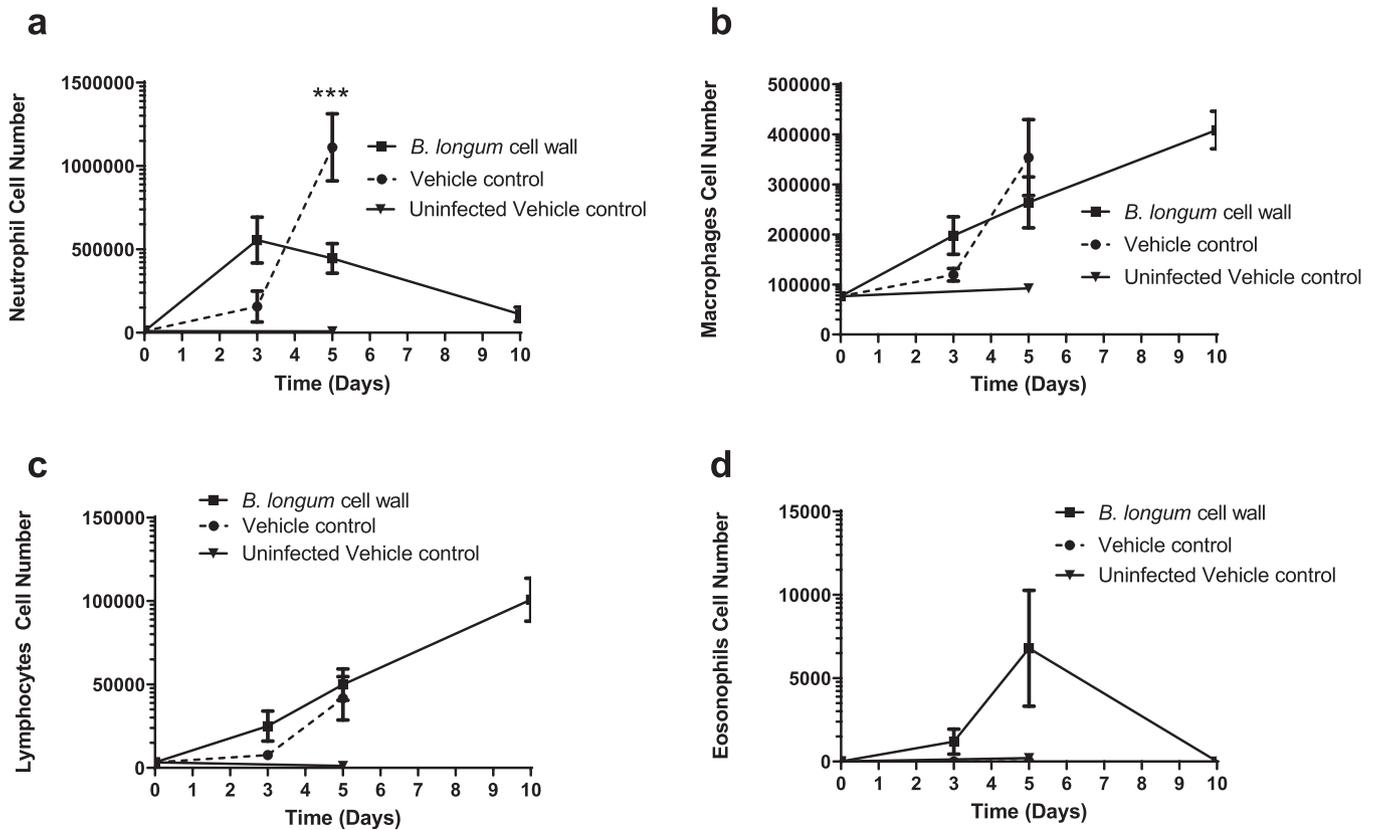
Fig. 2. *B. longum* **35624**®*-derived cell wall alters cellular recruitment to the lungs.*
Time-dependent changes in (**a**) neutrophil, (**b**) macrophage, (**c**) lymphocyte and (**d**) eosinophil levels in BAL fluid were influenced by viral infection and administration of bifidobacterial cell wall fraction. Data shown are mean ± SEM results of 5 animals per group for each time point. ***$p < 0.001$ (2-way ANOVA).

4. Discussion

The results show that an influenza infection that is uniformly lethal in mice can be abated by intra-nasal administration of an intact bacterial strain or an isolated cell-wall preparation of *B. longum* **35624**. Enhanced survival was associated with reduced viral replication in the lungs, a dose-dependent reduction in markers of lung damage, altered cellular infiltration and cytokines in BAL. Non-specific interference with the viral infection was excluded because protection was also evident when the bifidobacterial-derived cell wall preparation was administered post-viral inoculation.

Influenza viruses are highly transmissible and effects on the host can vary from mild symptoms to fatal disease. Despite over 100 years of research, knowledge of the precise pathogenesis, optimal vaccines and appropriate specific treatments remain elusive albeit with significant advances in oxygen therapy, mechanical ventilation, antivirals, and antibiotics [16]. A successful antiviral response usually involves rapid localised secretion of pro-inflammatory cytokines and interferons (IFNs) to limit viral replication accompanied by appropriate activation of NK cells, innate lymphoid cells (ILCs), neutrophils and monocytes [17,18]. However, if this response is delayed or insufficient then sustained activation of these innate immune cells occurs that can cause catastrophic damage within the lungs [18,19].

Resolution of virus-induced innate-mediated inflammation requires migration of dendritic cells, macrophages and adaptive immune cells to infected sites [19-21].

The murine model utilised in this report replicates these features of influenza virus-induced immune pathology whereby viral load increases dramatically within 5 days, which is associated with elevated innate immune cells (especially neutrophils), cytokines, cell death, vascular damage and ultimately leads to death [22]. Macrophages and lymphocytes dominated the lavages of mice in the *B.*

longum cell wall treated group that survived up to 10 days following infection.

The rationale for considering *bifidobacteria* as a strategy for host defense against respiratory viral infections is primarily based on their recorded modulatory effects on innate and acquired immunity in humans and experimental animals [9-12,15,23]. While the majority of human studies have been conducted following oral administration, beneficial effects of probiotics in non-gastrointestinal infections have also been observed [24]. Several bacterial strains have been confirmed to exert protective effects against influenza infection in murine models after oral administration, including *B. longum* [25], *Lactobacillus casei* [26], and *Lactobacillus pentosus* [27]. In addition, nasal administration of viable or non-viable probiotics such as *Lactobacillus casei* Shirota, *Lactobacillus pentosus* S-PT84 and *Lactobacillus rhamnosus* GG/ CRL1505 can improve cellular responses against influenza infection [28-31]. The responsible mechanisms were shown to be associated with an increase in IFN-γ or the type I IFNs [25,26,29-37]. In contrast, we show that improved survival and reduced viral titres are associated with decreased IFN-γ and type I IFNs, suggesting a novel mechanism of action.

The most well-defined antiviral responses include the type I IFNs, IFN-α and IFN-β, but their pathologic potential has also been observed, particularly in the setting of acute influenza infection [38]. Type I IFN-driven inflammatory features in patients with severe influenza were recently documented leading to a proposal that the type I IFN response can play a pivotal role in exacerbating inflammation [39]. In this context, it is noteworthy that the bifidobacterial-mediated responses in the present study were associated with a significant reduction in interferons α and β in BAL samples when compared with controls. Similarly, reduced levels of the downstream cytokines stimulated by type I IFNs, such as IL-6, IFN-γ, and the chemokines IP-10 (also known as CXCL-10) and MCP-1 (CCL2) were

Vehicle Control

a

(left column label: 3 days)

40μm

b *B. longum* cell wall

40μm

c

(left column label: 5 days)

40μm

d

40μm
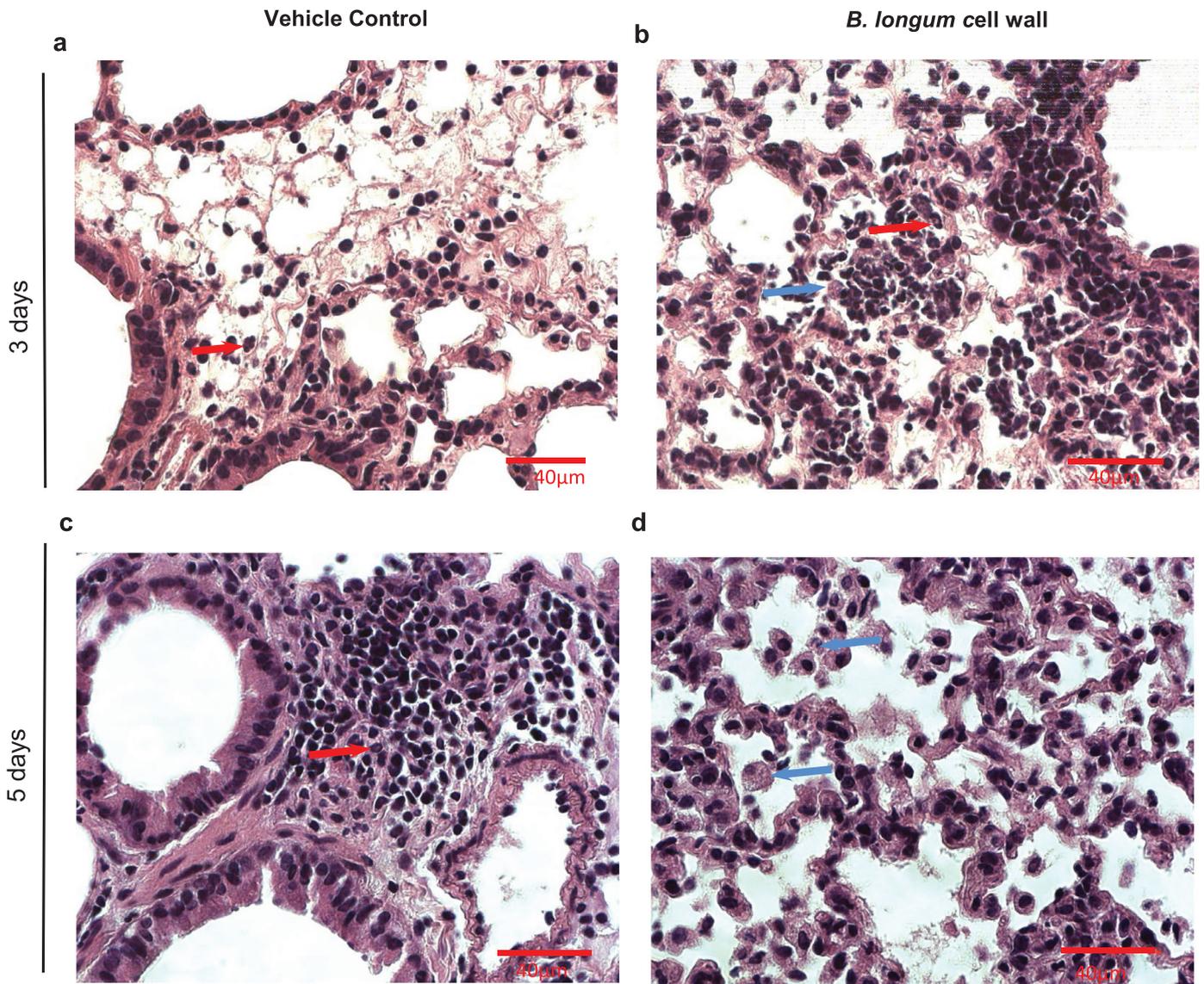
Fig. 3. *Influenza infection and immune cell infiltration in lung tissue sections.*
    Selected photomicrographs (600x) of formalin-fixed, paraffin-embedded lung tissue sections stained with H&E from (**a**) animals receiving vehicle control alone at day 3 post-influenza inoculation; (**b**) *B. longum* cell wall-treated animals at day 3 post-influenza inoculation; (**c**) animals receiving vehicle control alone at day 5 post-influenza inoculation; (**d**) *B. longum* cell wall-treated animals at day 5 post-influenza inoculation. Neutrophils (red arrows) and macrophages (blue arrows) are identified in the selected photomicrographs. Scale bar=40 μM.

observed. IL-6, IFN-γ, IP-10 and MCP-1 have been shown to be elevated in people infected with influenza [40-43]. In experimental models, blockade of IFN-γ and IP-10 with monoclonal antibodies ameliorates virus-induced lung injury [44,45].

While the optimal immune response to respiratory viral infections has yet to be defined, interferon-λ is known to participate in limiting viral replication and tissue damage. Interferon-λ (also known as IFNls, type III IFNs or IL-28 and IL-29) constitute a class of interferons sharing homology, expression patterns, and antiviral functions with the type I IFNs IFN-α and IFN-β [46,47]. Interferon-λ induces downstream signaling cascades similar to that of type I IFNs, driving the expression of interferon-stimulated genes (ISGs) and the induction of antiviral responses [48,49]. We observed that the levels of IFN-λ were significantly increased in BAL samples of bifidobacterial-derived cell wall treated mice at day 3 after influenza infection. Of note, IFN-λ has been reported to restrict viral replication without inducing pro-inflammatory responses or immunopathology [50-53]. Thus, the protective factor within the bifidobacterial cell wall may reduce type I IFN damaging responses due to promoting appropriate type III IFN

responses for anti-viral defense, although this mechanism will need to be further explored in future studies.

The bifidobacterial-derived cell wall fraction induced a dose-dependent increase in surfactant protein D (SP-D). SP-D is an innate sensor and contributor to anti-viral defense. SP-D has been reported to inhibit viral entry into epithelial cells and enhances phagocytosis and pulmonary clearance of influenza virus [54-56]. It acts, in part, by binding to viral mannose-rich glycans [57-59]. SP-D mediates a range of antiviral activities *in vitro*, including neutralization of virus infectivity and inhibition of the enzymatic activity of the viral neuraminidase, and SP-D-deficient mice were more susceptible to infection with highly glycosylated influenza viruses [56,57,59-62]. Thus, SP-D may be an additional important component mediating the bifidobacterial-induced benefits within the lung.

Differences in illness severity to a specific viral infection are thought to reflect variations in the host immune response. The current study suggests that these host response features are significantly influenced by exposure to certain microbes or their associated components. Recent studies in viral infection models using BALB/C mice
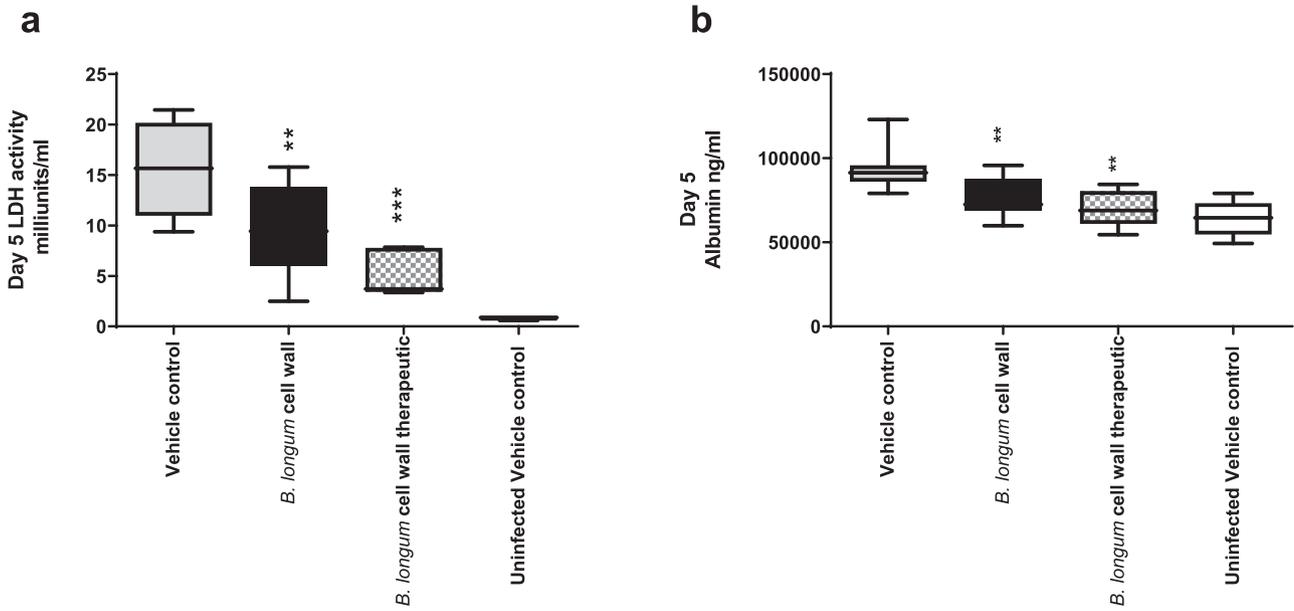
Fig. 4. *B. longum* **35624**® *-derived cell wall reduces lung cell death and vascular leakage.*
BAL LDH (**a**) and albumin (**b**) levels were analysed at day 5 post-influenza innoculation in animals receiving vechicle control alone, those administered the bifidobacterial-derived cell wall fraction starting 2 h before influenza inoculation (*B. longum* cell wall) or those animals administered the bifidobacterial-derived cell wall fraction starting 24 h after influenza inoculation (*B. longum* cell wall therapeutic) or uninfected controls. Data are presented as box-and-whisker plots with the median values and maximum/minimum values illustrated of 10 animals per group. $^*p < 0.05$; $^{**}p < 0.01$ (1-way ANOVA).
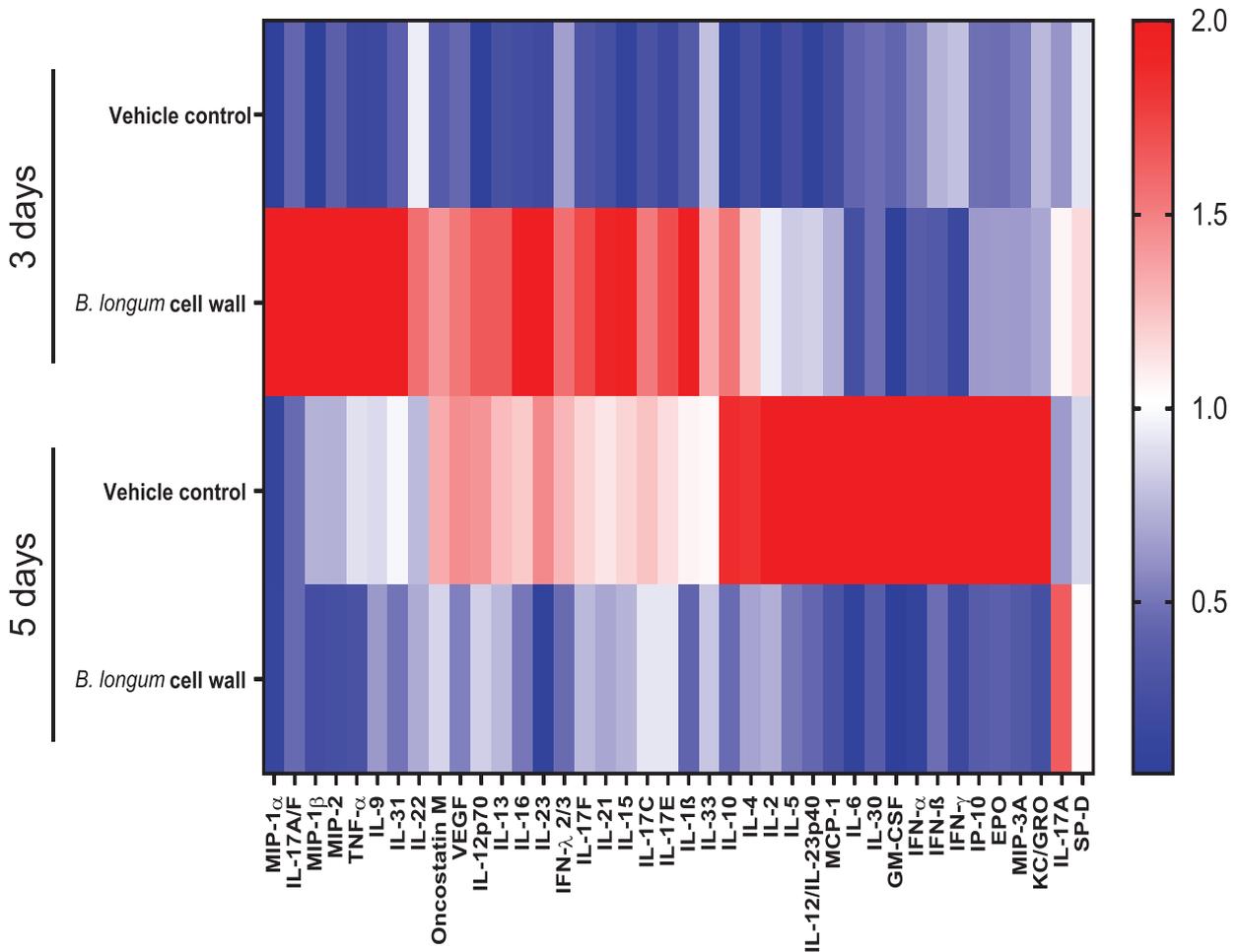
Fig. 5. *B. longum* **35624**® *-derived cell wall alters the cytokine profile of BAL.*
Heatmap representing increasing levels (blue to red) of the BAL cytokines, chemokines and surfactant protein D (SP-D) for each group at two time points (3 days or 5 days post inoculation with influenza). Peak fold change in cytokine levels was normalized by dividing the sum of the mean of fold change observed in the vehicle group.
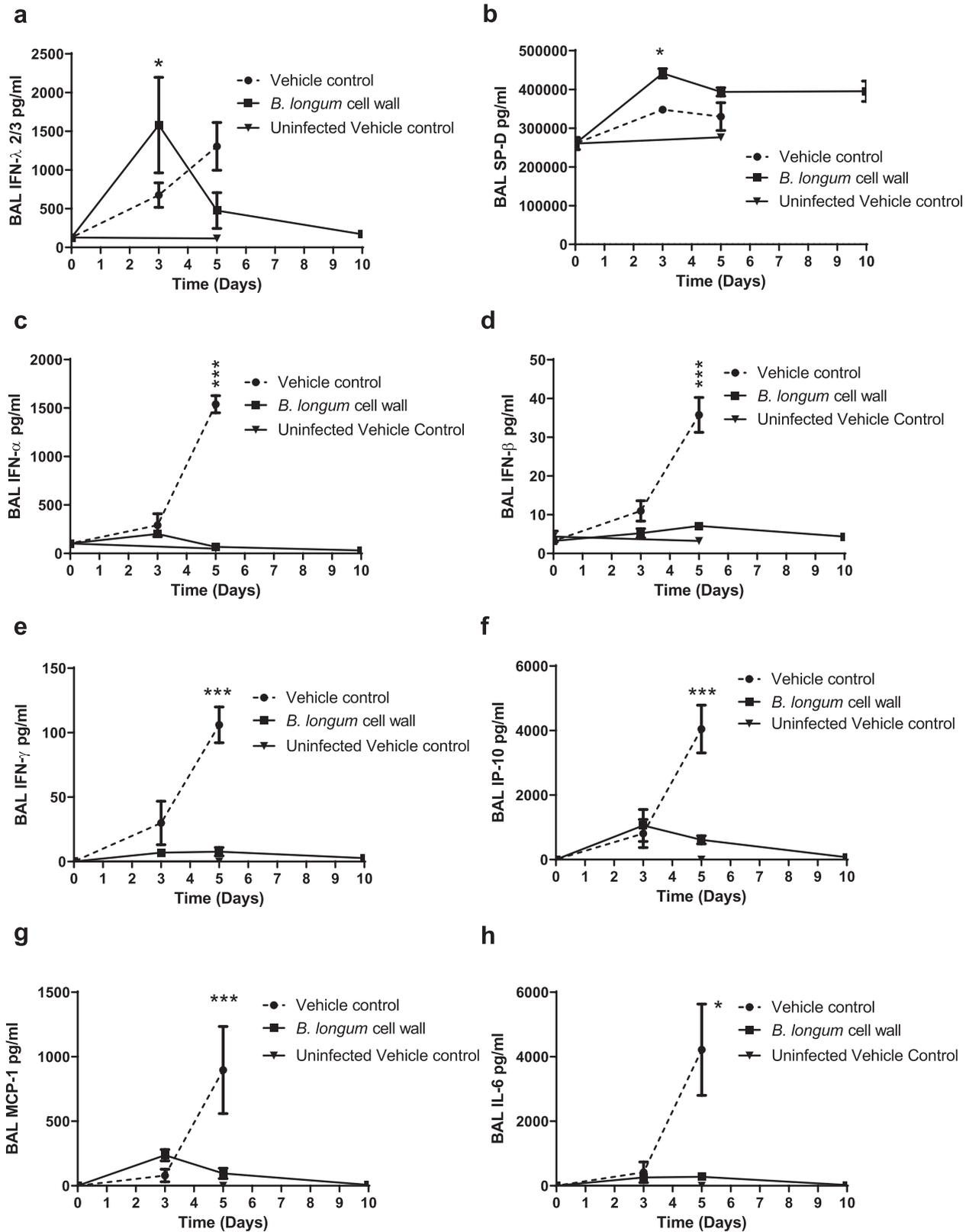
Fig. 6. *Time course profiles of surfactant protein D and cytokines in BAL from influenza infected mice.*

Concentrations in BAL at days 3, 5 and 10 days post-viral innoculation for (**a**) IFN-λ2/3, (**b**) surfactant protein D (SP-D), (**c**) IFN-α, (**d**) IFN-β, (**e**) IFN-γ (**f**) IP-10, (**g**) MCP-1, and (**h**) IL-6 were determined by Multiplex assay. Data shown are mean $\pm$ SEM results of 5 animals per group for each time point. $^*p < 0.05$; $^{***}p < 0.001$ (2-way ANOVA).

suggest that the relative timing of the type 1 IFN responses and maximal virus replication is a key determinant of outcome [63,64]. While the dynamic nature of the cytokine and chemokine responses was evident in the present study using BALB/C mice, it is particularly noteworthy that the beneficial effect of intra-nasal bifidobacterial treatment was evident regardless of whether it was administered before or after the onset of infection, but optimal timing of administration needs to be further defined.
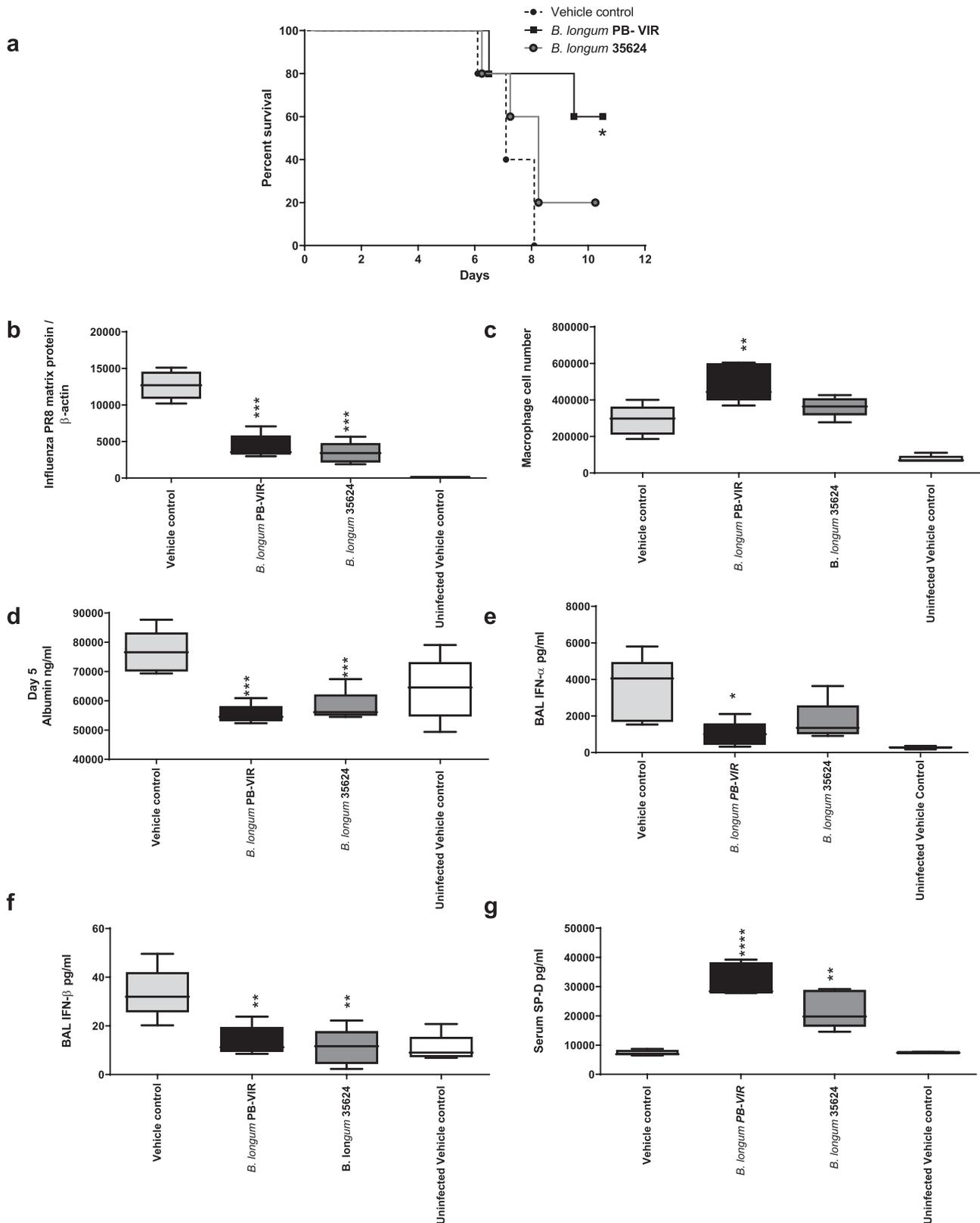
Fig. 7. *B. longum* **PB-VIR^TM** *protects against lethal influenza infection.*

(**a**) Survival was evaluated up to 10 days post inoculation (*n* = 5 animals per group). *$p < 0.05$ (log-rank Mantel-Cox test). (**b**) Viral load was measured at day 5 post-infection by quantitative real-time PCR. Data are presented as box-and-whisker plots with the median values and maximum/minimum values illustrated (*n* = 5 animals per group). ***$p < 0.01$ (1-way ANOVA). (**c**) Macrophage counts in BAL fluid were compared at days 5 post innoculation. Data are presented as box-and-whisker plots with the median values and maximum/minimum values illustrated (*n* = 5 animals per group). **$p < 0.01$ (1-way ANOVA). (**d**) BAL albumin levels were analysed at day 5 post-influenza innoculation as determined by ELISA. Data are presented as box-and-whisker plots with the median values and maximum/minimum values illustrated (*n* = 5 animals per group)..***$p < 0.001$ (1-way ANOVA). Concentrations in BAL at day 5 post viral innoculation for (**e**) IFN-α, (**f**) IFN-β, and serum (**g**) SP-D were determined by Multiplex assay. Data are presented as box-and-whisker plots with the median values and maximum/minimum values illustrated (*n* = 5 animals per group). *$p < 0.05$; **$p < 0.01$,. ****$p < 0.0001$ (1-way ANOVA).

Probiotic effects are most commonly considered in the context of protection against bacterial infections and disturbances of the intestinal microbiome, such as in irritable bowel syndrome [12,65], but our results support the prospect of a role in prevention or treatment of viral infections in the lung. Moreover, safety, ease of administration by topical application and comparatively low cost, are particularly appealing. The encouraging results of intra-nasal administration of *B. longum* **PB-VIR**[TM], *B. longum* **35624** and its cell wall derived fraction in a model of lethal murine influenza infection with the mouse adapted PR8 strain, suggests that this strategy should be examined in future human studies, particularly against seasonal influenza infections. However, optimal strain selection, product format and route of administration for use in humans for this particular indication will require more research including logistical as well biological considerations.

Author contributions

DG, RG, BK, DM, RW, SB, EMH, CAA and LOM conceived, planned, and oversaw the studies. DG, ES, RG, and MKL performed laboratory experiments. DG, RG, MKL, and LOM performed data analysis. DG, FS, and LOM interpreted the data and wrote the paper. All authors contributed to reviewing the paper and all authors agreed to the final version for submission.

Declaration of Competing Interest

DG and BK are employees of PBG. ES, RG were employees of AHPD. DM, RW, SB, and EMH are full-time employees of GSK and hold company stock. CAA has received grants from Allergopharma, Idorsia, Swiss National Science Foundation, Christine Kühne-Center for Allergy Research and Education, European Commission's Horison's 2020 Framework Programme, Cure, Novartis Research Institutes, Astra Zeneca, Scibase, and GSK. CAA is on the advisory board of Sanofi & Regeneron. FS is a founder shareholder of the following university campus companies: Atlantia Food Clinical Trials Ltd and Tucana Ltd now known as 4D pharma Cork. FS also is a science advisor to Kaleido Biosciences. LOM has consulted for PBG and has received research funding from GSK.

Supplementary materials

Supplementary material associated with this article can be found, in the online version, at doi:10.1016/j.ebiom.2020.102981.

References

[1] Spadaro S, Park M, Turrini C, et al. Biomarkers for acute respiratory distress syndrome and prospects for personalised medicine. J Inflamm (Lond) 2019;16:1.

[2] Barcik W, Pugin B, Bresco MS, et al. Bacterial secretion of histamine within the gut influences immune responses within the lung. Allergy 2019;74(5):899–909.

[3] Hagan T, Cortese M, Rouphael N, et al. Antibiotics-driven gut microbiome perturbation alters immunity to vaccines in humans. Cell 2019;178(6) 1313-28 e13.

[4] Michalovich D, Rodriguez-Perez N, Smolinska S, et al. Obesity and disease severity magnify disturbed microbiome-immune interactions in asthma patients. Nat Commun 2019;10(1):5711.

[5] Sencio V, Barthelemy A, Tavares LP, et al. Gut dysbiosis during influenza contributes to pulmonary pneumococcal superinfection through altered short-chain fatty acid production. Cell Rep 2020;30(9):2934–47 e6.

[6] Sokolowska M, Frei R, Lunjani N, Akdis CA, O'Mahony L. Microbiome and asthma. Asthma Res Pract 2018;4:1.

[7] Tsang TK, Lee KH, Foxman B, et al. Association between the respiratory microbiome and susceptibility to influenza virus infection. Clin Infect Dis 2019.

[8] Wypych TP, Wickramasinghe LC, Marsland BJ. The influence of the microbiome on respiratory health. Nat Immunol 2019;20(10):1279–90.

[9] Groeger D, O'Mahony L, Murphy EF, et al. Bifidobacterium infantis 35624 modulates host inflammatory processes beyond the gut. Gut Microbes 2013;4(4):325–39.

[10] Konieczna P, Groeger D, Ziegler M, et al. Bifidobacterium infantis 35624 administration induces Foxp3 T regulatory cells in human peripheral blood: potential role for myeloid and plasmacytoid dendritic cells. Gut 2012;61(3):354–66.

[11] O'Mahony C, Scully P, O'Mahony D, et al. Commensal-induced regulatory T cells mediate protection against pathogen-stimulated NF-kappaB activation. PLoS Pathog 2008;4(8):e1000112.

[12] O'Mahony L, McCarthy J, Kelly P, et al. Lactobacillus and bifidobacterium in irritable bowel syndrome: symptom responses and relationship to cytokine profiles. Gastroenterology 2005;128(3):541–51.

[13] Altmann F, Kosma P, O'Callaghan A, et al. Genome analysis and characterisation of the exopolysaccharide produced by Bifidobacterium longum subsp. longum 35624. PLoS ONE 2016;11(9):e0162983.

[14] Schiavi E, Gleinser M, Molloy E, et al. The surface-associated exopolysaccharide of Bifidobacterium longum 35624 plays an essential role in dampening host proinflammatory responses and repressing local TH17 responses. Appl Environ Microbiol 2016;82(24):7185–96.

[15] Schiavi E, Plattner S, Rodriguez-Perez N, et al. Exopolysaccharide from Bifidobacterium longum subsp. longum 35624 modulates murine allergic airway responses. Benef Microbes 2018;9(5):761–73.

[16] Dunning J, Thwaites RS, Openshaw PJM. Seasonal and pandemic influenza: 100 years of progress, still much to learn. Mucosal Immunol 2020;13(4):566–73.

[17] Dunning J, Blankley S, Hoang LT, et al. Progression of whole-blood transcriptional signatures from interferon-induced to neutrophil-associated patterns in severe influenza. Nat Immunol 2018;19(6):625–35.

[18] Monticelli LA, Sonnenberg GF, Abt MC, et al. Innate lymphoid cells promote lung-tissue homeostasis after infection with influenza virus. Nat Immunol 2011;12 (11):1045–54.

[19] Cole SL, Ho LP. Contribution of innate immune cells to pathogenesis of severe influenza virus infection. Clin Sci (Lond) 2017;131(4):269–83.

[20] Grant EJ, Quinones-Parra SM, Clemens EB, Kedzierska K. Human influenza viruses and CD8(+) T cell responses. Curr Opin Virol 2016;16:132–42.

[21] La Gruta NL, Turner SJ. T cell mediated immunity to influenza: mechanisms of viral control. Trends Immunol 2014;35(8):396–402.

[22] Newton AH, Cardani A, Braciale TJ. The host immune response in respiratory virus infection: balancing virus clearance and immunopathology. Semin Immunopathol 2016;38(4):471–82.

[23] Konieczna P, Ferstl R, Ziegler M, et al. Immunomodulation by Bifidobacterium infantis 35624 in the murine lamina propria requires retinoic acid-dependent and independent mechanisms. PLoS ONE 2013;8(5):e62617.

[24] Panigrahi P, Parida S, Nanda NC, et al. A randomized synbiotic trial to prevent sepsis among infants in rural India. Nature 2017;548(7668):407–12.

[25] Kawahara T, Takahashi T, Oishi K, et al. Consecutive oral administration of Bifidobacterium longum MM-2 improves the defense system against influenza virus infection by enhancing natural killer cell activity in a murine model. Microbiol Immunol 2015;59(1):1–12.

[26] Hori T, Kiyoshima J, Shida K, Yasui H. Augmentation of cellular immunity and reduction of influenza virus titer in aged mice fed Lactobacillus casei strain Shirota. Clin Diagn Lab Immunol 2002;9(1):105–8.

[27] Kiso M, Takano R, Sakabe S, et al. Protective efficacy of orally administered, heat-killed Lactobacillus pentosus b240 against influenza A virus. Sci Rep 2013;3:1563.

[28] Zelaya H, Tada A, Vizoso-Pinto MG, et al. Nasal priming with immunobiotic Lactobacillus rhamnosus modulates inflammation-coagulation interactions and reduces influenza virus-associated pulmonary damage. Inflamm Res 2015;64 (8):589–602.

[29] Hori T, Kiyoshima J, Shida K, Yasui H. Effect of intranasal administration of Lactobacillus casei Shirota on influenza virus infection of upper respiratory tract in mice. Clin Diagn Lab Immunol 2001;8(3):593–7.

[30] Izumo T, Maekawa T, Ida M, et al. Effect of intranasal administration of Lactobacillus pentosus S-PT84 on influenza virus infection in mice. Int Immunopharmacol 2010;10(9):1101–6.

[31] Harata G, He F, Hiruta N, et al. Intranasal administration of Lactobacillus rhamnosus GG protects mice from H1N1 influenza virus infection by regulating respiratory immune responses. Lett Appl Microbiol 2010;50(6):597–602.

[32] Yasui H, Kiyoshima J, Hori T. Reduction of influenza virus titer and protection against influenza virus infection in infant mice fed Lactobacillus casei Shirota. Clin Diagn Lab Immunol 2004;11(4):675–9.

[33] Kawase M, He F, Kubota A, Harata G, Hiramatsu M. Oral administration of lactobacilli from human intestinal tract protects mice against influenza virus infection. Lett Appl Microbiol 2010;51(1):6–10.

[34] Takeda S, Takeshita M, Kikuchi Y, et al. Efficacy of oral administration of heat-killed probiotics from Mongolian dairy products against influenza infection in mice: alleviation of influenza infection by its immunomodulatory activity through intestinal immunity. Int Immunopharmacol 2011;11(12):1976–83.

[35] Lee YN, Youn HN, Kwon JH, et al. Sublingual administration of Lactobacillus rhamnosus affects respiratory immune responses and facilitates protection against influenza virus infection in mice. Antiviral Res 2013;98(2):284–90.

[36] Maeda N, Nakamura R, Hirose Y, et al. Oral administration of heat-killed Lactobacillus plantarum L-137 enhances protection against influenza virus infection by stimulation of type I interferon production in mice. Int Immunopharmacol 2009;9(9):1122–5.

[37] Nakayama Y, Moriya T, Sakai F, et al. Oral administration of Lactobacillus gasseri SBT2055 is effective for preventing influenza in mice. Sci Rep 2014;4:4638.

[38] Davidson S, Crotta S, McCabe TM, Wack A. Pathogenic potential of interferon alphabeta in acute influenza infection. Nat Commun 2014;5:3864.

[39] Lee JS, Park S, Jeong HW, et al. Immunophenotyping of COVID-19 and influenza highlights the role of type I interferons in development of severe COVID-19. Sci Immunol 2020;5(49).

[40] Califano D, Furuya Y, Roberts S, Avram D, McKenzie ANJ, Metzger DW. IFN-gamma increases susceptibility to influenza A infection through suppression of group II innate lymphoid cells. Mucosal Immunol 2018;11(1):209–19.

[41] Coates BM, Staricha KL, Koch CM, et al. Inflammatory Monocytes Drive Influenza A Virus-Mediated Lung Injury in Juvenile Mice. J Immunol 2018;200(7):2391–404.

[42] Ichikawa A, Kuba K, Morita M, et al. CXCL10-CXCR3 enhances the development of neutrophil-mediated fulminant lung injury of viral and nonviral origin. Am J Respir Crit Care Med 2013;187(1):65–77.

[43] Paquette SG, Banner D, Zhao Z, et al. Interleukin-6 is a potential biomarker for severe pandemic H1N1 influenza A infection. PLoS ONE 2012;7(6):e38214.

[44] Liu B, Bao L, Wang L, et al. Anti-IFN-gamma therapy alleviates acute lung injury induced by severe influenza A (H1N1) pdm09 infection in mice. J Microbiol Immunol Infect 2019.

[45] Wang W, Yang P, Zhong Y, et al. Monoclonal antibody against CXCL-10/IP-10 ameliorates influenza A (H1N1) virus induced acute lung injury. Cell Res 2013;23(4):577–80.

[46] Lazear HM, Nice TJ, Diamond MS. Interferon-lambda: immune functions at barrier surfaces and beyond. Immunity 2015;43(1):15–28.

[47] Wack A, Terczynska-Dyla E, Hartmann R. Guarding the frontiers: the biology of type III interferons. Nat Immunol 2015;16(8):802–9.

[48] Durbin RK, Kotenko SV, Durbin JE. Interferon induction and function at the mucosal surface. Immunol Rev 2013;255(1):25–39.

[49] Mendoza JL, Schneider WM, Hoffmann HH, et al. The IFN-lambda-IFN-lambdaR1-IL-10Rbeta complex reveals structural features underlying type III IFN functional plasticity. Immunity 2017;46(3):379–92.

[50] Davidson S, McCabe TM, Crotta S, et al. IFNlambda is a potent anti-influenza therapeutic without the inflammatory side effects of IFNalpha treatment. EMBO Mol Med 2016;8(9):1099–112.

[51] Forero A, Ozarkar S, Li H, et al. Differential activation of the transcription factor IRF1 underlies the distinct immune responses elicited by type I and type III interferons. Immunity 2019;51(3):451–64 e6.

[52] Galani IE, Triantafyllia V, Eleminiadou EE, et al. Interferon-lambda Mediates Non-redundant Front-Line Antiviral Protection against Influenza Virus Infection without Compromising Host Fitness. Immunity 2017;46(5):875–90 e6.

[53] Kim S, Kim MJ, Kim CH, et al. The superiority of IFN-lambda as a therapeutic candidate to control acute influenza viral lung infection. Am J Respir Cell Mol Biol 2017;56(2):202–12.

[54] Thiel S, Reid KB. Structures and functions associated with the group of mammalian lectins containing collagen-like sequences. FEBS Lett 1989;250(1):78–84.

[55] Sastry K, Ezekowitz RA. Collectins: pattern recognition molecules involved in first line host defense. Curr Opin Immunol 1993;5(1):59–66.

[56] LeVine AM, Whitsett JA, Hartshorn KL, Crouch EC, Korfhagen TR. Surfactant protein D enhances clearance of influenza A virus from the lung in vivo. J Immunol 2001;167(10):5868–73.

[57] Hartshorn KL, White MR, Shepherd V, Reid K, Jensenius JC, Crouch EC. Mechanisms of anti-influenza activity of surfactant proteins A and D: comparison with serum collectins. Am J Physiol 1997;273(6):L1156–66.

[58] Hartshorn KL, White MR, Voelker DR, Coburn J, Zaner K, Crouch EC. Mechanism of binding of surfactant protein D to influenza A viruses: importance of binding to haemagglutinin to antiviral activity. Biochem J 2000;351(Pt 2):449–58.

[59] Reading PC, Morey LS, Crouch EC, Anders EM. Collectin-mediated antiviral host defense of the lung: evidence from influenza virus infection of mice. J Virol 1997;71(11):8204–12.

[60] Hawgood S, Brown C, Edmondson J, et al. Pulmonary collectins modulate strain-specific influenza a virus infection and host responses. J Virol 2004;78(16):8565–72.

[61] Tecle T, White MR, Crouch EC, Hartshorn KL. Inhibition of influenza viral neuraminidase activity by collectins. Arch Virol 2007;152(9):1731–42.

[62] Vigerust DJ, Ulett KB, Boyd KL, Madsen J, Hawgood S, McCullers JA. N-linked glycosylation attenuates H3N2 influenza viruses. J Virol 2007;81(16):8593–600.

[63] Channappanavar R, Fehr AR, Vijay R, et al. Dysregulated type I interferon and inflammatory monocyte-macrophage responses cause lethal pneumonia in SARS-CoV-infected mice. Cell Host Microbe 2016;19(2):181–93.

[64] Channappanavar R, Fehr AR, Zheng J, et al. IFN-I response timing relative to virus replication determines MERS coronavirus infection outcomes. J Clin Invest 2019;130:3625–39.

[65] Whorwell PJ, Altringer L, Morel J, et al. Efficacy of an encapsulated probiotic Bifidobacterium infantis 35624 in women with irritable bowel syndrome. Am J Gastroenterol 2006;101(7):1581–90.